RSC Advances

ROYAL SOCIETY OF CHEMISTRY

www.rsc.org/advances

Cite this: DOI: 10.1039/c0xx00000x

www.rsc.org/xxxxxx

ARTICLE TYPE

Novel Visible-Light Driven g-C_3N_4/$Zn_{0.25}Cd_{0.75}S$ Composite Photocatalyst for Efficient Degradation of Dyes and Reduction of Cr(VI) in Water

Meng Sun,[a,b] Tao Yan,[c,d] Qing Yan[a], Hongye Liu[c], Liangguo Yan[a], Yongfang Zhang[a] and Bin Du*[,a]

Received (in XXX, XXX) XthXXXXXXXXX 20XX, Accepted Xth XXXXXXXXX 20XX
DOI: 10.1039/b000000x

Abstract: A facile and template free in situ precipitation method was developed for the synthesis of g-C_3N_4/$Zn_{0.25}Cd_{0.75}S$ photocatalyst. The obtained products were characterized by X-ray diffraction (XRD), transmission electron microscopy (TEM), high-resolution transmission electron microscopy (HRTEM), and ultraviolet-visible diffuse reflection spectroscopy (DRS). The DRS results showed that with the increase of g-C_3N_4 content, the light absorption edge for g-C_3N_4/$Zn_{0.25}Cd_{0.75}S$ was blue shifted in the visible light region. The TEM images showed that the $Zn_{0.25}Cd_{0.75}S$ particles had been finely distributed on the surfaces of g-C_3N_4 sheets. The HRTEM images showing clear lattice fringes proved the formation of heterojunction structure at the interfaces of g-C_3N_4 and $Zn_{0.25}Cd_{0.75}S$. In the photocatalytic degradation of dyes, g-C_3N_4/$Zn_{0.25}Cd_{0.75}S$ composite exhibited significantly enhanced activities, and the optimal g-C_3N_4 content was 20 wt%. A controlled experiment showed that the high charge separation efficiency of the photo-generated electron–hole pairs and the suitable energy band structures result in the high performance of g-C_3N_4/$Zn_{0.25}Cd_{0.75}S$ under visible light irradiation. The g-C_3N_4/$Zn_{0.25}Cd_{0.75}S$ sample also possessed a superior activity in the photocatalytic reduction of Cr(VI) in neutral solution. The photoelectrochemical measurement confirmed that the interface charge separation efficiency was greatly improved by coupling g-C_3N_4 with $Zn_{0.25}Cd_{0.75}S$. Terephthalic acid photoluminescence probing technique has been performed to detect the generation of •OH in the reaction system.

Keywords: Photocatalysis; g-C_3N_4/$Zn_{0.25}Cd_{0.75}S$; Degradation

Introduction

Nowadays, toxic organic pollutants composed of synthetic textile dyes and other industrial dyestuffs become one of the main sources of water pollution. All those pollutants discharged from factories are harmful to the environment and human health. More severely, they are difficult to remove by traditional treatment method because of the high stability.[1-3]Most of the azo dyes and fluorine dyes, such as aromatic amines, are suspected to have carcinogenic effects, so the international environmental standards are becoming more and more stringent, correspondingly the treatment of organic pollutants discharged into the environment has also been developed recently.[4,5] As we all know, the photocatalytic oxidation (PCO) technology was an effective method for the environment remediation.[6-10] Titanium dioxide (TiO_2) has been widely studied as a photocatalyst for pollutant degradation and solar energy conversion.[11-14] However, its large band gap (3.2 eV for anatase) and low quantum yield determine that it is only active under ultraviolet light irradiation.[15] Therefore, great efforts have been devoted to suppressing the recombination rate of photo-generated carriers and exploring visible-light driven photocatalyst.[16,17]

Recently, great efforts have been done in our group to explore visible-light responsive photocatalysts. For example, Li et al., has reported the synthesis and visible light photocatalytic activity of $Zn_xCd_{1-x}S$ solid solutions.[18]Through changing the molar ratio of Zn/Cd in the preparation process, $Zn_xCd_{1-x}S$ nanocrystals with different band-gaps have been obtained. The molar ratio of Zn/Cd in $Zn_xCd_{1-x}S$ has great influences on its activity under visible light illumination. And it was found that the sample with molar ratio of Zn/Cd = 1:3 ($Zn_{0.25}Cd_{0.75}S$) displayed the best activity. In order to further improve the activity of $Zn_{0.25}Cd_{0.75}S$, it has been used to combine with TiO_2 to synthesize $Zn_{0.25}Cd_{0.75}S/TiO_2$ composite photocatalyst for improving the carrier separation efficiency, but the results were not satisfactory.[19]

In this paper, we have used graphitic carbon nitride (g-C_3N_4) to

[a]*School of Resources and Environment, University of Jinan, Shandong Provincial Engineering Technology Research Center for Ecological Carbon Sink and Capture Utilization, Jinan250022, P.R. China. Fax: +86 531-82765969; Tel:+86 531-82769235;E-mail:binduujn@163.com*
[b]*Fujian Provincial Key Laboratory of Photocatalysis-State Key Laboratory Breeding Base, Fuzhou University, Fuzhou 350002, P.R. China*
[c]*School of Civil Engineering and Architecture, University of Jinan, Jinan250022, P.R. China.*
[d]*School of Chemistry, Beijing Institute of Technology, Beijing 100081, P.R. China*

combine with $Zn_{0.25}Cd_{0.75}S$ to prepare efficient visible-light responsive g-C_3N_4/$Zn_{0.25}Cd_{0.75}S$ composite photocatalyst. Similar with graphene[20-22], g-C_3N_4 has received considerable attention due to its wide applications. The photocatalytic performance of g-C_3N_4 was first reported by Wang et al., but its activity was really low under visible light irradiation.[23]In this work, we have demonstrated a facile in situ precipitation method to synthesize g-C_3N_4/$Zn_{0.25}Cd_{0.75}S$ composite with high photocatalytic activity toward methyl orange (MO) and rhodamine B (RhB) under visible light irradiation. It was found that the g-C_3N_4 content had great influences on the photocatalytic activity, and the optimum g-C_3N_4 mass ratio was 20%. Moreover, g-C_3N_4/$Zn_{0.25}Cd_{0.75}S$ photocatalyst also possessed a superior activity in the photocatalytic reduction of Cr(VI) in neutral solution without addition of any sacrifice reagents.

Experimental section

Synthesis of g-C_3N_4

All the reagents are analytical-grade and purchased from Sinopharm Chemical Reagent Co., Ltd. The g-C_3N_4 powders were synthesized by heating melamine in a muffle furnace according to the literatures with small modification.[24,25] Briefly, 5 g of melamine was put into a semi-closed alumina crucible with a cover. The crucible was then placed in a muffle furnace and heated to 500 °C at a heating rate of 5 °C min^{-1}, which has been held for 3 h at this temperature. When the temperature of alumina crucible was cooled down after reaction, the obtained g-C_3N_4 products would be ground into powders for use.

Synthesis of g-C_3N_4/$Zn_{0.25}Cd_{0.75}S$

The facile in situ synthesis routes are as follows: first, an appropriate amount of analytical grade $Zn(Ac)_2{\cdot}2H_2O$ and $Cd(Ac)_2{\cdot}2H_2O$ (Zn/Cd = 1:3) were dissolved in deionized water to form a solution. Then a certain amount of g-C_3N_4 powders were added into this solution, which was then poured into Teflon-lined container (100 mL) and ultrasonicated for 30 min to completely disperse the g-C_3N_4. After that, a certain amount of 0.5 M Na_2S solution was slowly added into the suspension with continuous stirring. After being stirred for 12 h at room temperature, the Teflon-lined container was then sealed in a stainless steel autoclave and maintained at 160 °C for 16 h. After reaction, the autoclave was naturally cooled to ambient temperature, and the obtained solid products were centrifuged, washed and dried in air at 80 °C overnight. According to this method, g-C_3N_4/$Zn_{0.25}Cd_{0.75}S$ composite photocatalysts with different mass ratios of 5, 10, 20, 30, 40, 50, and 60 wt% have been synthesized and named as CNZS-5, CNZS-10, CNZS-20, CNZS-30, CNZS-40, CNZS-50, and CNZS-60, respectively. PM-g-C_3N_4/$Zn_{0.25}Cd_{0.75}S$ is the abbreviation for the g-C_3N_4/$Zn_{0.25}Cd_{0.75}S$ composite prepared by the physical mixing method with a same composition as CNZS-20 (20 wt% g-C_3N_4 and 80 wt% $Zn_{0.25}Cd_{0.75}S$ physical mixed without any treatment). Pure CdS, g-C_3N_4/ZnS (20 wt%), and g-C_3N_4/CdS (20 wt%) composites have also be fabricated as references.

Characterization of photocatalysts

X-ray diffraction (XRD) patterns of the obtained products were recorded on a Bruker D8 Advance X-ray diffractometer under the conditions of generator voltage = 40 kV; generator current = 40 mA; divergence slit = 1.0 mm; Cu Kα (λ = 1.5406 Å); and polyethylene holder. The TEM and HRTEM images were obtained on a JEOL model JEM 2010 EX transmission electron microscope. Diffuse reflectance ultraviolet–visible light (UV–vis) spectra (DRS) were measured at room temperature in the range of 200–700 nm on a UV–vis spectrophotometer (Cary 500 Scan Spectrophotometers, Varian, and U.S.A) equipped with an integrating sphere attachment. CHI-660D electrochemical workstation (CH Instruments, USA) has been used to perform the photoelectrochemical experiment. A three-electrode cell equipped with a quartz window has been used for the photoelectrochemical current response measurements. The sample deposited FTO glass has been used as the working electrode. The counter and reference electrodes were platinum wire and Ag/AgCl electrode, respectively. The electrolyte used in the experiment was 0.02 M Na_3PO_4 solution.

Photocatalytic tests

The visible light activity of g-C_3N_4/$Zn_{0.25}Cd_{0.75}S$ composites were evaluated by the photocatalytic degradation of dyes (MO and RhB) in aqueous solution. A 500 W halogen lamp (Philips Electronics) has been used as the visible light source, which was placed in a cylindrical glass vessel equipped with water cooling system. The temperature of the reaction system has been maintained at 25 ºC. Two cut-off filters have been used to completely remove any radiation below 420 nm, ensuring only visible light (420 nm < λ < 800 nm) could penetrate and irradiate the reaction system. 80 mL of MO aqueous solution (10 ppm) was first added into a 100 mL Pyrex glass vessel, and then 0.08 g of the obtained sample was introduced to form a suspension. Before visible-light irradiation, the suspension was stirred for 60 min for the dye and catalyst to reach adsorption–desorption equilibrium. During the reaction process under visible light irradiation, 3 mL aliquots were sampled at given time intervals. The acquired suspension was centrifuged to remove the catalyst, and the resulting clear liquor was analyzed using a Perkin-Elmer UV-vis spectrophotometer to monitor the dye concentrations. The percentage for dye degradation has been reported as C/C_0. C is the absorption intensity for the main spectrum peak of dye at each irradiated time interval. And C_0 is the absorption intensity of the starting concentration when adsorption-desorption equilibrium was achieved. For comparison, N-doped TiO_2, In_2S_3, and CdS were utilized as references of visible-light driven photocatalysts. N-doped TiO_2 was synthesized by heating commercial P25 under NH_3 atmosphere at 600°C for 3 h.[26] CdS and In_2S_3 also have been respectively prepared according to previous literatures.[27,28] The experiment conditions for the photocatalytic reduction of Cr(VI) over g-C_3N_4/$Zn_{0.25}Cd_{0.75}S$ was nearly the same as that used in decomposing dyes except for the amount of catalyst added (40 mg/L) and the concentration of $K_2Cr_2O_7$ (50 mg/L).

Results and discussion

Structural characterization

Figure 1 showed the XRD patterns of the as-preparedg-C_3N_4, $Zn_{0.25}Cd_{0.75}S$, and g-C_3N_4/$Zn_{0.25}Cd_{0.75}S$ composites with different mass ratios. As we can see, The pure g-C_3N_4 sample has two distinct peaks located at 27.4° and 13.1° respectively, which are

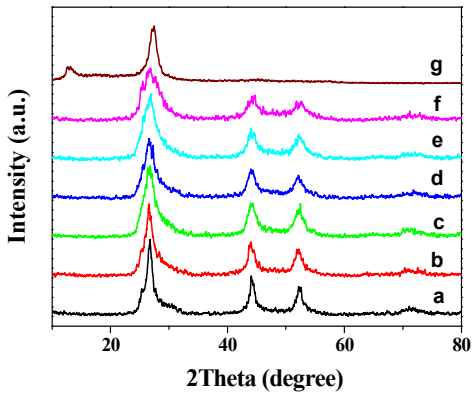

Figure 1. XRD patterns of pureg-C_3N_4, $Zn_{0.25}Cd_{0.75}S$, and g-C_3N_4/$Zn_{0.25}Cd_{0.75}S$ composite, (a) pure $Zn_{0.25}Cd_{0.75}S$, (b) CNZS-40, (c) CNZS-30, (d) CNZS-20, (e) CNZS-10, (f) CNZS-5, and (g) pure g-C_3N_4.

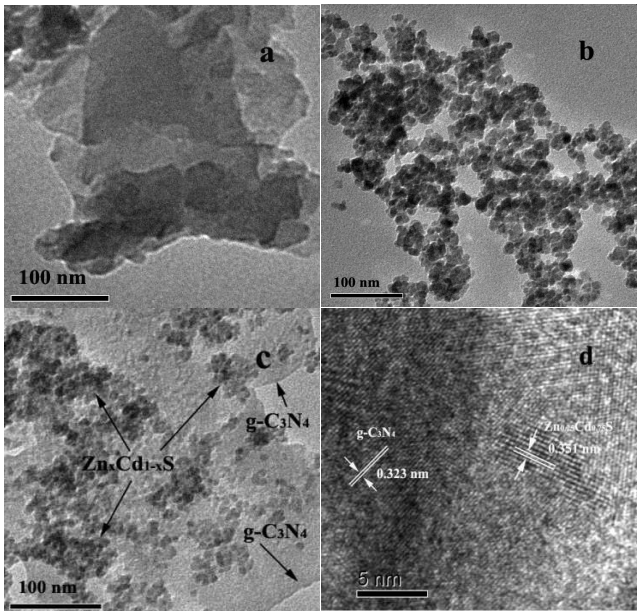

Figure 2.TEM micrographs of the samples, (a) pure g-C_3N_4, (b) pure $Zn_{0.25}Cd_{0.75}S$, (c) CNZS-20, and (d) HRTEM image of CNZS-20.

indexed to the (0 0 2) and (1 0 0) diffraction planes of g-C_3N_4 (JCPDS 87-1526). As for pure $Zn_{0.25}Cd_{0.75}S$, the sharp and narrow diffraction peaks demonstrate the good crystallization. However, for the g-C_3N_4/$Zn_{0.25}Cd_{0.75}S$ composites with different mass ratios, only broadened diffraction peaks for $Zn_{0.25}Cd_{0.75}S$ have been observed. The overlapping of the tow closely peaks for $Zn_{0.25}Cd_{0.75}S$ (26.7°) and g-C_3N_4 (27.4°) had made it difficult to distinguish the peak for g-C_3N_4. Ge et al. has reported a very similar phenomenon in fabricating g-C_3N_4/Bi_2WO_6 composite.[29]

The morphologies of g-C_3N_4, $Zn_{0.25}Cd_{0.75}S$, and g-C_3N_4/$Zn_{0.25}Cd_{0.75}S$ composites are demonstrated in Figure 2. Figure 2a revealed that the as-prepared g-C_3N_4 appears to be aggregated large sheets. Figure 2b showed that the as-prepared $Zn_{0.25}Cd_{0.75}S$ exhibited irregular particle morphology with a uniform diameter of 15 nm. Figure 2c illustrated that the $Zn_{0.25}Cd_{0.75}S$ particles had been finely distributed on the surfaces of g-C_3N_4 sheets. Figure 2d showed the HRTEM image of CNZS-20 sample. Two different kinds of lattice fringes were clearly exhibited, one of d = 0.323 nm matched (0 0 2) crystallographic plane of g-C_3N_4 (JCPDS 87-1526), the other of d = 0.351 nm matched the crystallographic plane of $Zn_{0.25}Cd_{0.75}S$, which was just between *d*= 0.362 nm for (1 0 0) planes (CdS in PDF No. 41-1049) and *d*= 0.311 nm for (1 1 1) planes (ZnS in PDF No. 65-0309). This finding suggested that the heterojunction structure was indeed formed in the g-C_3N_4/$Zn_{0.25}Cd_{0.75}S$ composites. The heterojunction interfaces would presumably provide good potential for carrier transport.

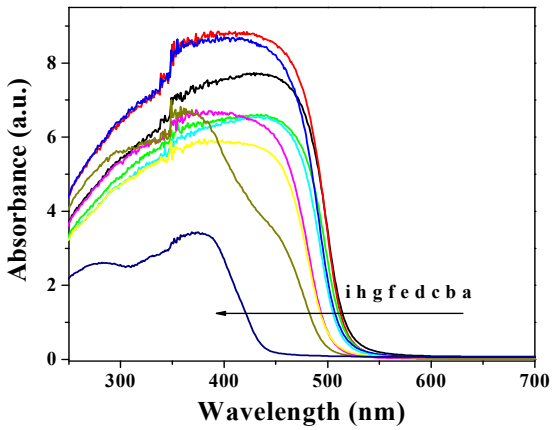

Figure 3. UV–vis diffuse reflectance spectra of the as-prepared samples: (a) pure $Zn_{0.25}Cd_{0.75}S$, (b) CNZS-5, (c) CNZS-10, (d) CNZS-20, (e) CNZS-30, (f) CNZS-40, (g) CNZS-50, (h) CNZS-60, and (i) pure g-C_3N_4.

Optical characterization

The UV–vis diffuse reflectance spectra of g-C_3N_4, $Zn_{0.25}Cd_{0.75}S$, and g-C_3N_4/$Zn_{0.25}Cd_{0.75}S$ composites were shown in Figure 3. As we can see, the light absorption of the samples is different. The absorption edge of g-C_3N_4 was estimated at 450 nm, while that for $Zn_{0.25}Cd_{0.75}S$ was located at 510 nm. As for the g-C_3N_4/$Zn_{0.25}Cd_{0.75}S$ composites, their visible light absorption red-shifted which might result in generation of more electron-hole pairs and therefore enhancement of photocatalytic activity.

Photocatalytic activity tests

The activities of g-C_3N_4/$Zn_{0.25}Cd_{0.75}S$ composites were mainly evaluated by the visible light photocatalytic degradation for dyes and reduction of Cr(VI). The temporal concentration changes of dye, such as MO, were monitored by examining the variations in maximal absorption in UV–vis spectra at 464 nm. To investigate the influences of g-C_3N_4 content on the photocatalytic activity, g-C_3N_4/$Zn_{0.25}Cd_{0.75}S$ composites with different g-C_3N_4 contents were used to decompose MO under the same conditions, and the results were shown in Figure 4.As we can see, pure $Zn_{0.25}Cd_{0.75}S$ showed a poor activity, that the degradation ratio of MO was only 33% after 75 min of visible light irradiation, while pure g-C_3N_4 could hardly decompose MO. However, when a small amount of g-C_3N_4 was combined with $Zn_{0.25}Cd_{0.75}S$, the activity would be remarkably enhanced. We estimate the optimum g-C_3N_4 mass ratio was 20%. When the g-C_3N_4 mass ratio gradually increased from 5 to 20%, the photocatalytic degradation ratio of MO was correspondingly improved from 66 to 99% within 45 min of reaction. However, when the g-C_3N_4 content was further increased, the photocatalytic activities of g-C_3N_4/$Zn_{0.25}Cd_{0.75}S$ composites decreased gradually. For example, when the g-C_3N_4 content increased to 60%, the MO degradation ratio decreased to

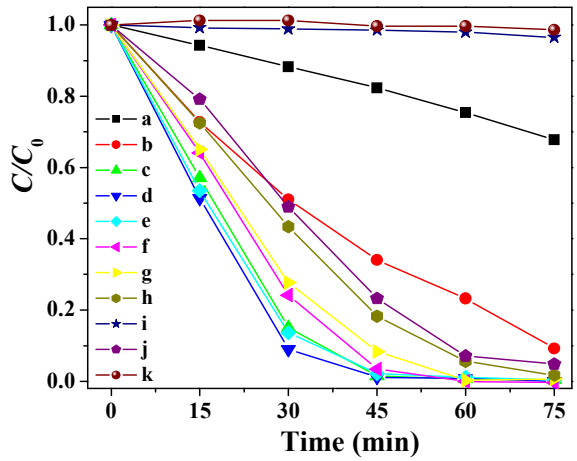

Figure 4. Degradation rates of MO under visible light irradiation using (a) pure $Zn_{0.25}Cd_{0.75}S$, (b) CNZS-5, (c) CNZS-10, (d) CNZS-20, (e) CNZS-30, (f) CNZS-40, (g) CNZS-50, (h) CNZS-60, (i) pure g-C_3N_4, (j) g-C_3N_4/CdS(20wt%), and (k) g-C_3N_4/ZnS(20wt%).

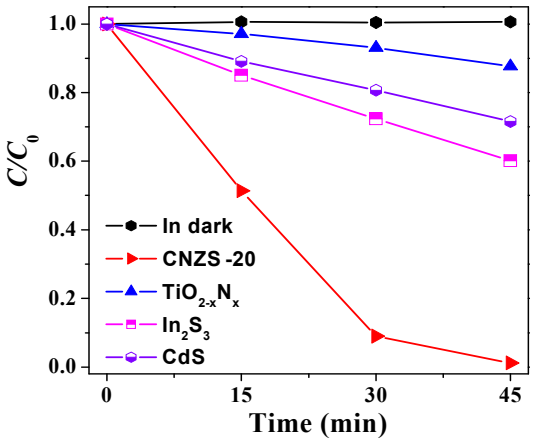

Figure 5. Comparisons of photodegradation of MO on CNZS-20, $TiO_{2-x}N_x$, CdS, and In_2S_3 under identical conditions.

82%. It was noteworthy that the activity of CNZS-20 was indeed higher than that for g-C_3N_4/CdS (20 wt%).

To evaluate the photocatalytic activities of g-C_3N_4/$Zn_{0.25}Cd_{0.75}S$ composites, other photocatalyst such as $TiO_{2-x}N_x$, CdS, and In_2S_3 was respectively used as comparison to decompose MO under visible light irradiation. Figure 5 showed that when the suspension containing CNZS-20 catalyst was stirred in the dark for 45 min, no obvious concentration change of MO has been observed. However, under visible light irradiation, the photocatalytic activity of CNZS-20 was greatly higher than that of CdS, In_2S_3, and $TiO_{2-x}N_x$. After 45 min of reaction, the decomposition ratio of MO over CNZS-20 was up to 99%, while CdS, In_2S_3, and $TiO_{2-x}N_x$ only decomposed 29, 40, and 12% of MO dye respectively.

Furthermore, CNZS-20 has also exhibited excellent photocatalytic activity in decomposing RhB (2×10^{-5} M) under visible light irradiation. The temporal concentration changes of RhB were monitored by examining the variations in maximal absorption at 554 nm, and the degradation results were shown in Figure 6. As we can see, RhB could be quickly decomposed under visible light illumination over CNZS-20, and about 99% could be degraded within 45 min. As a comparison, the degradation of RhB over PM-g-C_3N_4/$Zn_{0.25}Cd_{0.75}S$ was also investigated under the same conditions, and the degradation results were also shown in Figure 6. It can be clearly seen that the activity of PM-g-C_3N_4/$Zn_{0.25}Cd_{0.75}S$ is getting worse compared with pure $Zn_{0.25}Cd_{0.75}S$. That is to say, even if g-C_3N_4 and

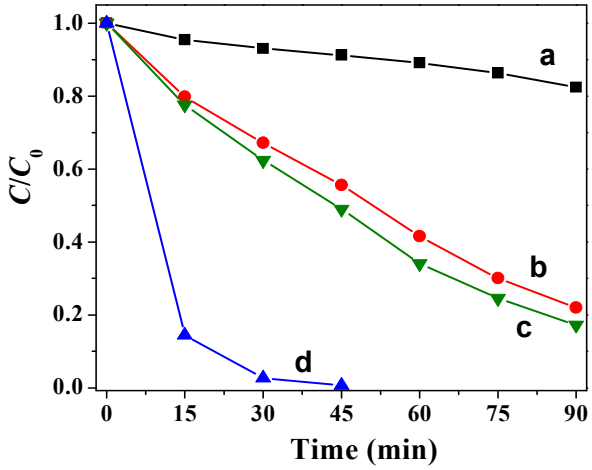

Figure 6. Degradation rates of RhB under visible light irradiation using (a) pure g-C_3N_4, (b) PM-g-C_3N_4/$Zn_{0.25}Cd_{0.75}S$, (c) pure $Zn_{0.25}Cd_{0.75}S$, and (d) CNZS-20.

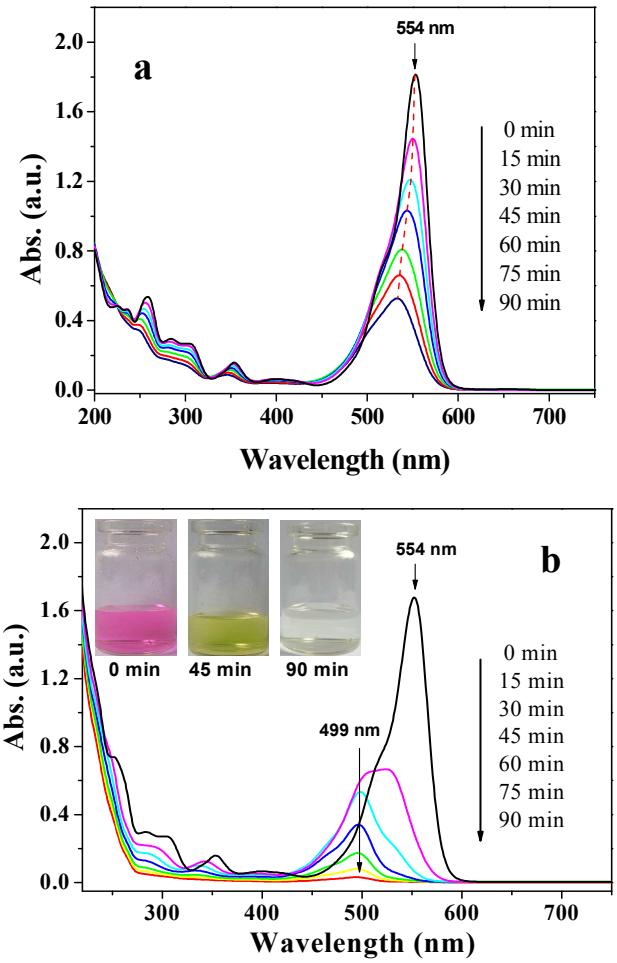

Figure 7. The absorption spectra of RhB in the presence of (a) pure $Zn_{0.25}Cd_{0.75}S$ and (b) CNZS-20 under exposure to visible light (420 nm < λ < 800 nm).

$Zn_{0.25}Cd_{0.75}S$ was physically mixed together in the ratio of 2:8, the activity was not enhanced because there no heterojunction interface was formed with simply physical mixing.

Figure 7 showed the temporal evolution of the spectral changes of RhB mediated by CNZS-20 and $Zn_{0.25}Cd_{0.75}S$, respectively. It exhibited that the degradation processes of RhB over CNZS-20 and $Zn_{0.25}Cd_{0.75}S$ were different. In the presence of $Zn_{0.25}Cd_{0.75}S$, the absorption peak of RhB located at 554 nm gradually blue shifted and decreased in the whole degradation process. However, when CNZS-20 was mediated, the absorption peak of RhB quickly shifted from 554 to 499 nm within 30 min of reaction. This hypsochromic shift of absorption maximum was caused by the N-deethylation of RhB during irradiation, which has been confirmed by Watanabe and co-workers.[30,31]

The photocatalyst's lifetime is very important for its practical application. The repeated degradation experiments toward MO over CNZS-20 photocatalyst have been performed. In the cycle experiments, the photocatalyst was centrifuged and dried after each run, which was then weighed again to add the lost portion and used for the next run. The results were shown in Figure 8. It showed that there was no obvious loss of photocatalytic properties after the 4th run. The XRD patterns of the fresh and used CNZS-20 samples were also shown in Figure 9. It illustrated that the crystal structure of the CNZS-20 did not change after the photocatalytic reaction. Therefore, the CNZS-20 photocatalyst

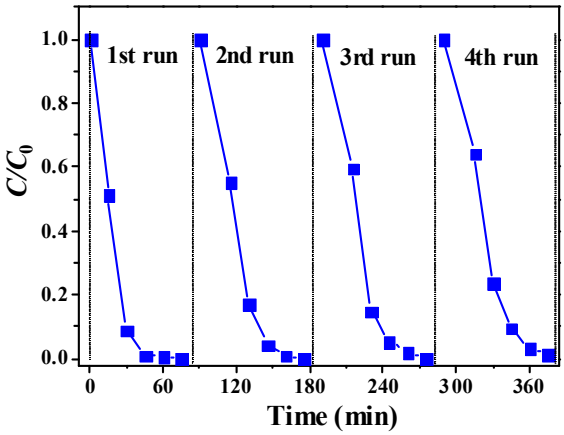

Figure 8. Cycling run in the photocatalytic degradation of MO over CNZS-20 sample.

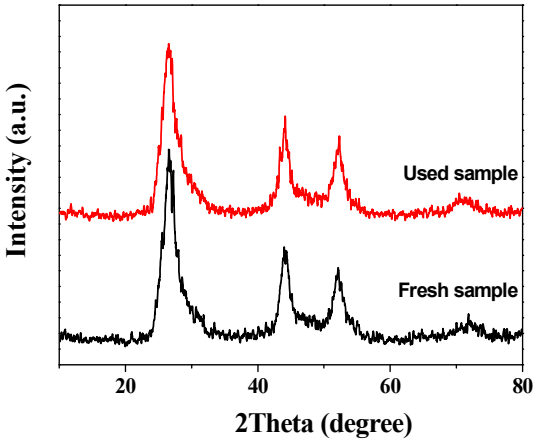

Figure 9. Comparison of XRD patterns between the fresh and used CNZS-20 sample.

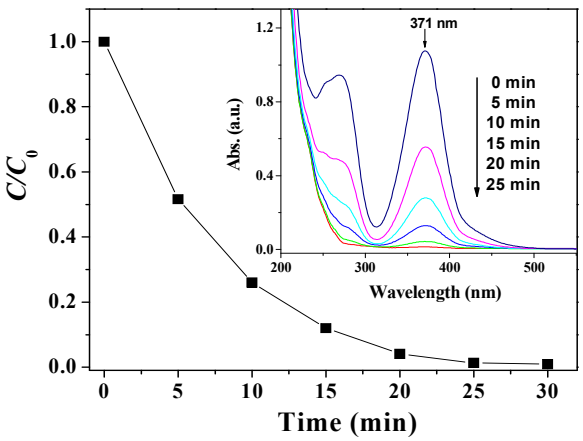

Figure 10. Photocatalytic reduction of aqueous Cr(VI) over CNZS-20 under visible light irradiation. (Inset) UV-visible spectral changes of Cr(VI) in aqueous CNZS-20 dispersions as a function of irradiation time.

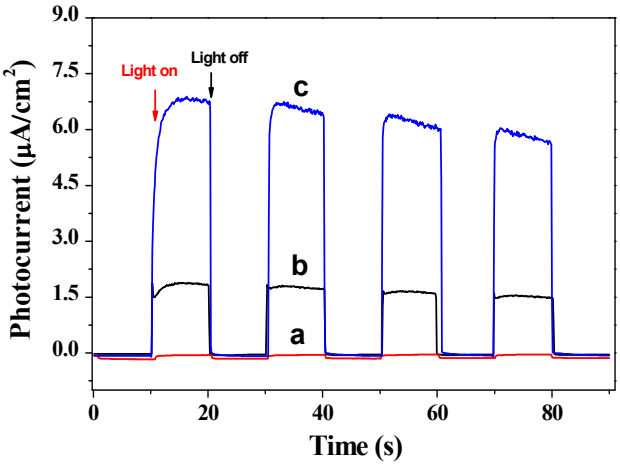

Figure 11. Photocurrent response of (a) pure g-C_3N_4, (b) $Zn_{0.25}Cd_{0.75}S$, and (c) CNZS-20 under visible light irradiation.

was stable enough and photo-corrosion hardly occurred in the reaction.

In addition, CNZS-20 photocatalyst also exhibited efficient activity for photocatalytic reduction of Cr(VI) to Cr(III) in neutral solution without any addition of sacrifice reagents. As shown in Figure 10, the maximum absorption band of the Cr(VI) solution located at 371 nm decreased gradually with the increase of irradiation time. After 25 min of reaction the absorption peak completely disappeared, and the reduction ratio of Cr(VI) was up to 99%. That is to say, because of the formation of heterojunction structure and high separation efficiency of carriers, large amount of electrons would be provided to deoxidize Cr(VI), while the holes might oxidize water to produce H^+ and O_2 when no extra hole scavengers were added in the system.

Because g-C_3N_4 was an effective electron transporter, it would facilitate the charge migration and reduce the recombination of electron–hole pairs for the g-C_3N_4 based photocatalysts. When heterojunction interface was formed between g-C_3N_4 and $Zn_{0.25}Cd_{0.75}S$, the photo-generated electrons should be quickly transfer from g-C_3N_4 to $Zn_{0.25}Cd_{0.75}S$, and consequently enhance the overall activity. To better understand this standpoint, photoelectrochemical technique was used to characterize g-C_3N_4, $Zn_{0.25}Cd_{0.75}S$, and CNZS-20 sample.

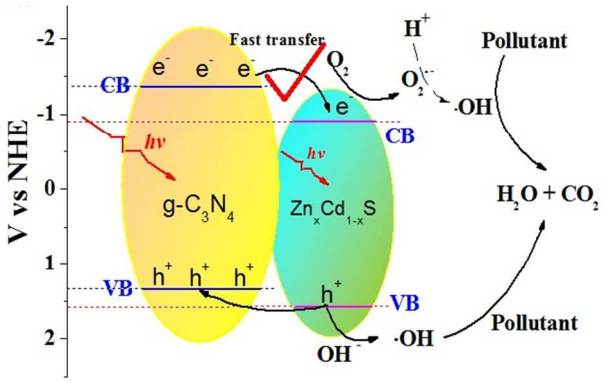

Figure 12. Proposed mechanism for the photocatalytic degradation of dyes on CNZS-20 under visible light irradiation.

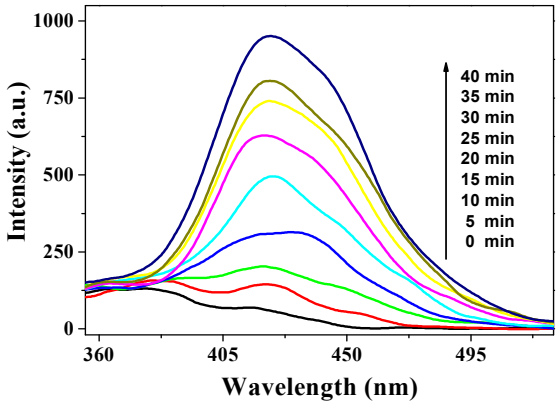

Figure 13. •OH-trapping PL spectra of suspensions containing CNZS-20 and TA.

Enhancement of interface charge separation efficiency

Figure 11 showed the photocurrent transient response for the electrodes of bare g-C_3N_4, $Zn_{0.25}Cd_{0.75}S$, and CNZS-20 under visible light irradiation. As it can be seen, with the light switched -on and -off cycles, the CNZS-20 sample exhibited the highest photocurrent transient response under visible light irradiation, which was greatly larger than that for bare g-C_3N_4 and $Zn_{0.25}Cd_{0.75}S$. It suggested the remarkably enhanced carrier separation ratio over CNZS-20, which was in agreement with the enhancement of photo-activity for CNZS-20.

The high separation efficiency of photo-generated carriers should be ascribed to the suitable band potentials of g-C_3N_4 and $Zn_{0.25}Cd_{0.75}S$. According to a previous report, $Zn_{0.25}Cd_{0.75}S$ was n-type semiconductor with V_{fb} of −0.8 V.[19] The conduction band potential (V_{CB}) of $Zn_{0.25}Cd_{0.75}S$ was about −0.9 V, while the valence band potential (V_{VB}) was 1.51 V. As for g-C_3N_4, Wang et al., reported that the V_{CB} and V_{VB} of polymeric g-C_3N_4 were determined at −1.3 and +1.4 V[23], respectively. A scheme for the separation and transport of photo-generated electron–hole pairs on the g-C_3N_4/$Zn_{0.25}Cd_{0.75}S$ interface was shown in Figure 12. The photo-induced electrons in g-C_3N_4 could move freely towards the surface of $Zn_{0.25}Cd_{0.75}S$ while the holes could transfer to the VB of g-C_3N_4 conveniently. As a result, the photo-generated electrons and holes were efficiently separated between g-C_3N_4 and $Zn_{0.25}Cd_{0.75}S$ thereby enhanced the photocatalytic activity. Hydroxyl radicals (•OH) were commonly considered as the possible key active species in the degradation process.[29,32,33]

Figure 13 showed the •OH-trapping PL spectra of suspensions containing CNZS-20 and terephthalic acid. It exhibited that the fluorescence intensity increased steadily along with the irradiation time. It elucidated that •OH in CNZS-20 system was really produced under visible light irradiation.

Conclusions

Novel visible-light induced g-C_3N_4/$Zn_{0.25}Cd_{0.75}S$ photocatalysts have been successfully synthesized via a facile in situ precipitation method. After introduction of g-C_3N_4, the g-C_3N_4/$Zn_{0.25}Cd_{0.75}S$ photocatalyst possessed a significantly enhanced visible light activity in decomposing dyes. The highest degradation efficiency was observed for the CNZS-20 sample. The activity enhancement was mainly attributed to the high separation efficiency of electron–hole pairs on their heterojunction interfaces. This method was expected to be extended for other g-C_3N_4 loaded materials, which might have potential applications in removing pollutants.

Acknowledgment

This work was financially supported by the Scientific Research Reward Fund for Excellent Young and Middle-Aged Scientists of Shandong Province (BS2012HZ001), National Natural Science Foundation of China (No. 21103069, 21075052, 21175057, and 40672158), and Scientific Research Foundation for Doctors of University of Jinan (XBS1037 and XKY1043).

References

1 S. Rengaraj, S. Venkataraj, J.W. Yeon, Y. Kim, X.Z. Li and G.K.H. Pang, *Appl. Catal. B: Environ.* 2007, **77**, 157.
2 J.S. Hu, L.L. Ren, Y.G. Guo, H.P. Liang, A.M. Cao, L.J. Wan and C.L. Bai, Angew. Chem. Int. Ed. 2005, **44**, 1269.
3 D.Z. Li, Z.X. Chen, Y.L. Chen, W.J. Li, H.J. Huang, Y.H. He and X.Z. Fu, *Environ. Sci. Technol*. 2008, 42, 2130.
4 H. Lachheb, E. Puzenat, A. Houas, M. Ksibi, E. Elaloui, C. Guillard and J.M. Herrmann, *Appl. Catal. B: Environ*. 2002, **39**, 75.
5 Z.X. Chen, D.Z. Li, W.J. Zhang, Y. Shao, T.W. Chen, M. Sun and X.Z. Fu, *J. Phys. Chem. C* 2009, **113**, 4433.
6 U.G. Akpan and B.H. Hameed, *J. Hazard. Mater*. 2009, **170**, 520.
7 N.S. Foster, R.D. Noble and C.A. Koval, *Environ. Sci. Technol.*1993, **27**, 350.
8 R. Vinu and G. Madras, Environ. Sci. Technol. 2008, 42, 913.
9 J.J. Testa, M.A. Grela and M.I. Litter, *Environ. Sci. Technol*. 2004, **38**, 1589.
10 S. Luo, Y. Xiao, L.Yang, C. Liu, F. Su and Y. Li, *Sep. Purif. Technol*. 2011, **79**, 85.
11 L.M. Wang, N. Wang, L.H. Zhu, H.W. Yu and H.Q. Tang, *J. Hazard. Mater*. 2008, **152**, 93.
12 C.R. Chenthamarakshan and K. Rajeshwar, *Langmuir* 2000, **16**, 2715.
13 H.B. Yu, S. Chen, X. Quan, H.M. Zhao and Y.B. Zhang, *Environ. Sci. Technol*. 2008, **42**, 3791.
14 N. Shaham-Waldmann and Y. Paz, *J. Phys. Chem. C* 2010, **114**, 18946.
15 Y.C. Zhang, J. Li, M. Zhang and D.D. Dionysiou, *Environ. Sci. Technol*. 2011, **45**, 9324.
16 M. Sun, D.Z. Li, Y. Zheng, W.J. Zhang, Y. Shao, Y.B. Chen, W.J. Li and X.Z. Fu, *Environ. Sci. Technol*. 2009, **43**, 7877.
17 M. Sun, D.Z. Li, Y.B. Chen, W. Chen, W.J. Li, Y.H. He and X.Z. Fu, *J. Phys. Chem. C* 2009, **113**, 13825.
18 W.J. Li, D.Z. Li, Z.X. Chen, H.J. Huang, M. Sun, Y.H. He and X.Z. Fu, *J. Phys. Chem. C* 2008, **112**, 14943.

19 W.J. Li, D.Z. Li, S.G. Meng, W. Chen, X.Z. Fu and S. Yu, *Environ. Sci. Technol.* 2011, **45**, 2987.

20 X.R. Wang, X.L. Li, L. Zhang, Y.K. Yoon, P.K. Weber, H.L. Wang, J. Guo and H.J. Dai, *Science* 2009, **324**, 768.

21 X.S. Li, W.W. Cai, J.H. An, S. Kim, J. Nah, D.X. Yang, R. Piner, A. Velamakanni, I. Jung, E. Tutuc, S.K. Banerjee, L. Colombo and R.S. Ruoff, *Science* 2009, **324**, 1312.

22 Y.B. Zhang, T.T. Tang, C. Girit, Z. Hao, M.C. Martin, A. Zettl, M.F. Crommie, Y.R. Shen and F. Wang, *Nature* 2009, **459**, 820.

23 X.C. Wang, K. Maeda, A. Thomas, K. Takanabe, G. Xin, J.M. Carlsson, K. Domen and M. Antonietti, *Nat. Mater*. 2009, **8**, 76.

24 G. Zhang, J. Zhang, M. Zhang and X. Wang, *J. Mater. Chem.* 2012, **22**, 8083.

25 J. Liu, T. Zhang, Z. Wang, G. Dawson and W. Chen, *J. Mater. Chem.* 2011, **21**, 14398.

26 H. Irie, Y. Watanabe and K. Hashimoto, *J. Phys. Chem. B* 2003, **107**, 5483.

27 S.L. Xiong, B.J. Xi and Y.T. Qian, *J. Phys. Chem. C* 2010, **114**, 14029.

28 X.Q. An, J.C. Yu, F. Wang, C.H. Li and Y.C. Li, *Appl. Catal. B: Environ*. 2013, **129**, 80.

29 L. Ge, C.C. Han and J. Liu, *Appl. Catal. B: Environ*. 2011, **108-109**, 100.

30 T. Watanabe, T. Takizawa and K. Honda, *J. Phys. Chem.* 1977, **81**, 1845.

31 T. Takizawa, T. Watanabe and K. Honda, *J. Phys. Chem.* 1978, **82**, 1391.

32 W. Liu, M.L. Wang , C.X. Xu, S.F. Chen, *Chem. Eng. J.* 2012, **209**, 386.

33 S.C. Yan, Z.S. Li, Z.G. Zou, *Langmuir* 2010, **26(6)**, 3894.

Novel Visible-Light Driven g-C_3N_4/$Zn_{0.25}Cd_{0.75}S$ Composite Photocatalyst for Efficient Degradation of Dyes and Reduction of Cr(VI) in Water

Meng Sun,[a,b] Tao Yan,[c,d] Qing Yan[a], Hongye Liu[c], Liangguo Yan[a], Yongfang Zhang[a] and Bin Du[*,a]

[a] School of Resources and Environment, University of Jinan, Shandong Provincial Engineering Technology Research Center for Ecological Carbon Sink and Capture Utilization, Jinan 250022, P.R. China. Fax: +86 531-82765969; Tel: +86 531-82769235; E-mail: binduujn@163.com

[b] Fujian Provincial Key Laboratory of Photocatalysis-State Key Laboratory Breeding Base, Fuzhou University, Fuzhou 350002, P.R. China

[c] School of Civil Engineering and Architecture, University of Jinan, Jinan 250022, P.R. China.

[d] School of Chemistry, Beijing Institute of Technology, Beijing 100081, P.R. China

Graphical abstract

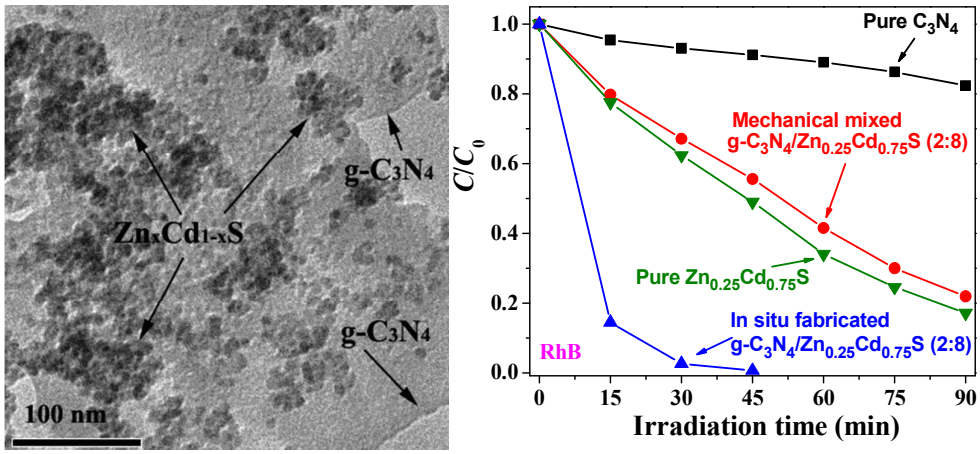

The formation of heterojunction structures at the interfaces of g-C_3N_4 and $Zn_{0.25}Cd_{0.75}S$ greatly enhanced the photocatalytic activity.